

Multi-line Stokes inversion for prominence magnetic-field diagnostics

R. Casini,¹ A. López Ariste,² F. Paletou,³ L. Léger³

¹*High Altitude Observatory, National Center for Atmospheric Research,¹ P.O. Box 3000, Boulder, CO 80307*

²*THÉMIS, CNRS UPS 853, C/Vía Láctea s/n, E-38200 La Laguna, Tenerife, Spain*

³*Laboratoire d'Astrophysique de Toulouse-Tarbes, Université de Toulouse, CNRS, 14 av. E. Belin, 31400 Toulouse, France*

ABSTRACT

We present test results on the simultaneous inversion of the Stokes profiles of the He I lines at 587.6 nm (D_3) and 1083.0 nm in prominences (90° scattering). We created datasets of synthetic Stokes profiles for the case of quiescent prominences ($B < 200$ G), assuming a conservative value of 10^{-3} of the peak intensity for the polarimetric sensitivity of the simulated observations. In this work, we focus on the error analysis for the inference of the magnetic field vector, under the usual assumption that the prominence can be assimilated to a slab of finite optical thickness with uniform magnetic and thermodynamic properties. We find that the simultaneous inversion of the two lines significantly reduces the errors on the inference of the magnetic field vector, with respect to the case of single-line inversion. These results provide a solid justification for current and future instrumental efforts with multi-line capabilities for the observations of solar prominences and filaments.

1. Introduction

The measurement of the vector magnetic field in solar prominences has become a priority goal to improve our understanding of the solar corona and its evolution. The long-term stability of quiescent prominences (from several days to several weeks) suggests that these structures of the solar atmosphere must be associated with a highly ordered topology of the magnetic field, right at the interface between the solar corona and the lower solar atmosphere. This long-term stability is not easily disrupted, despite the fact that the visible structure of quiescent prominences appears to be continually affected by highly dynamical events, like rising large-scale voids (*bubbles*) and ascending and descending small-scale plumes (de Toma et al. 2008; Berger et al. 2008). This is rather strong evidence that the stability of solar prominences—and its sudden disruption, when a

¹The National Center for Atmospheric Research is sponsored by the National Science Foundation.

quiescent prominence eventually erupts, leading to a coronal mass ejection (CME)—must somehow involve the magnetic topology of a much larger volume of the solar atmosphere than the actual visible structure, extending also to the prominence cavity and the corona above. That is why a concerted effort for measuring the magnetic field vector in prominences and in the solar corona is fundamental for the ultimate goal of understanding the manifestation of energetic events in the heliosphere, which are the main driver of space weather.

On the other hand, measurements of magnetic fields in prominences and in the corona are difficult. They impose very strict requirements on the instrumentation, and they require a deep understanding of the mechanisms of formation of line scattering polarization in a magnetized plasma. For this reason, only very recently the possibility of performing routine measurements of magnetic fields in prominences and in the corona has been given serious consideration, and new anticipated large-scale instruments (ATST, EST, COSMO,¹ SOLAR-C) are being developed specifically with this goal in mind.

On the interpretational side, the number of lines that are good diagnostics of prominence and coronal magnetic fields is quite restricted. For prominences, the primary choice has converged, over the past two or three decades, to the two lines of He I at 587.6 nm (D_3) and 1083.0 nm (10830). These two lines have been used at different times for studies of prominence magnetism (Leroy 1977; Querfeld et al. 1985; Paletou et al. 2001; Trujillo Bueno et al. 2002; Casini et al. 2003; Merenda et al. 2006; Kuckein et al. 2009). The long experience of the solar community in the magnetic inversion of photospheric lines has clearly demonstrated the advantage of multi-line polarimetric observations. The MTR observing mode available at the THÉMIS telescope (Paletou & Molodij 2001) is perfectly suited to accomplish such multi-line, spectro-polarimetric observations. Moreover, the implementation of optimized modulators, of new detectors with better efficiency in the near-infrared, and the use of the grid method of Semel (1980), allow since 2006 for the simultaneous and co-spatial observations of the two multiplets of He I in prominences. The HAO-NCAR Prominence Magnetometer (ProMag; Elmore et al. 2008), which is near completion, was specifically designed for this type of multi-line diagnostics.

It remains to prove that, for the specific case of the two He I lines, such diverse-wavelength diagnostics of prominence magnetism is indeed feasible, and that it would increase the reliability of the magnetic inversions. This is the motivation for the study presented in this paper. The feasibility of such multi-line approach to magnetic-field measurements in quiescent prominences is demonstrated through its preliminary application to simultaneous and co-spatial observations of these lines from THÉMIS. Thereafter, in order to demonstrate the robustness of this diagnostics, we performed a statistical analysis of the inversion errors over several databases of simulated observations. This analysis clearly shows the significance of the improvement in magnetic-field inversion by using both He I chromospheric lines.

¹<http://www.cosmo.ucar.edu>

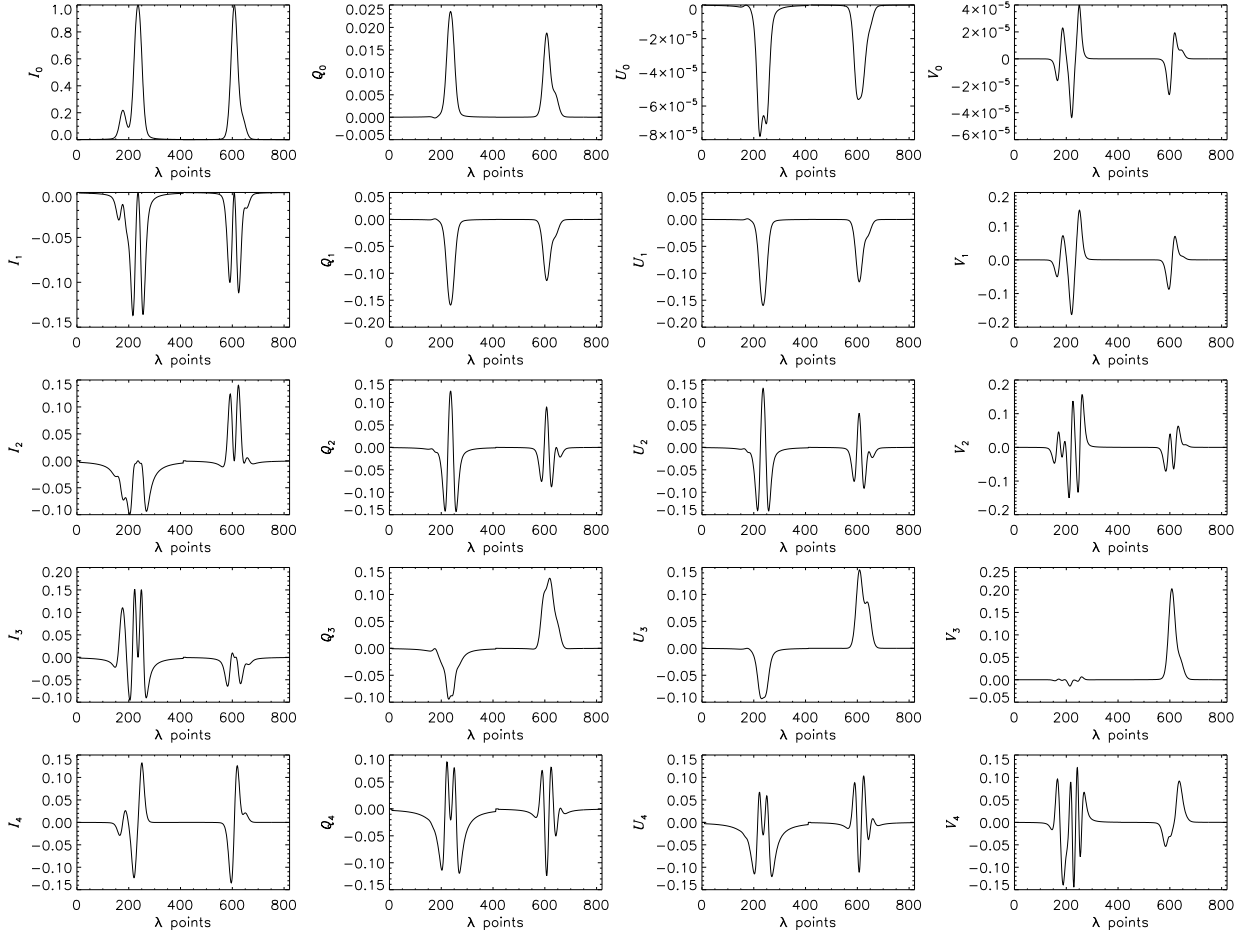


Fig. 1.— First four PCA eigenprofiles (rows 2 to 5) for the four Stokes parameters (I , Q , U , and V , from column 1 to 4, respectively) of the chromospheric lines He I 10830 (left profiles) and D₃ (right profiles) formed in an environment typical of quiescent prominences. The first row shows the mean Stokes profiles averaged over the entire parameter space spanned by our problem. The determination of the PCA eigenbasis from the merging of the spectral information of the two lines allows a clearer understanding of the physical correlations between the two lines with regards to the formation of their polarization signatures.

2. PCA strategy for multi-line inversion

The approach to magnetic inversion of line scattering polarization by Principal Component Analysis (PCA) of the Stokes profiles has been described elsewhere (López Ariste & Casini 2002; Casini, Bevilacqua, & López Ariste 2005). The inversion is performed by minimizing an appropriate Euclidean norm (*PCA distance*), which measures the deviation of the fitting profiles from the observations. This minimization is performed in the “dual space” of the PCA coefficients, which are the projections of the Stokes profiles onto a basis of *eigenprofiles* previously determined for

the problem at hand.² Since the PCA inversion is performed by searching for the best match of the observed profiles within a precomputed database of models, this method is very fast, and in addition is free from the risk of converging to local minima of the PCA distance.

Another advantage of the PCA approach to Stokes inversion is that all the essential spectro-polarimetric information about the line formation process, which is needed for a reliable inference of the magnetic and thermodynamic properties of the emitting plasma, is often encoded within a rather restricted set of eigenprofiles (typically between 3 and 6 components for each Stokes parameter, depending on the complexity of the line formation model). In fact, the most significant (i.e., low-order) PCA eigenprofiles often present patterns that can be directly ascribed to specific physical mechanisms intervening in the line formation process (Skumanich & López Ariste 2002). Thus the inspection of the eigenprofiles can help identify which mechanisms are at work in a particular polarized line profile. Often this identification is obvious, but sometimes the eigenprofiles can reveal the presence of correlations between spectral signatures that may not be evident in the original line profiles.

Figure 1 shows the first few PCA eigenprofiles for the two He I chromospheric lines. These were computed after merging the spectral information from the two lines into a fictitious single spectrum. This allows us to reveal correlations of polarized spectral features between the two lines, which we can reasonably expect must be present also in the line profiles of He I 10830 and D₃ formed under realistic conditions, but which may not be as evident from a study of the separate sets of eigenprofiles for the two lines.

The four columns in Fig. 1 show the PCA components of the Stokes parameters I , Q , U , and V , respectively. The first row shows the mean profiles averaged over the entire parameter space. As the magnetic field can attain all possible orientations, the average U and V Stokes profiles tend to zero, as expected. In fact, the good approximation to zero of those signals, as illustrated by Fig. 1, is an indication of the good coverage of the parameter space provided by the original database of line profiles, which was used for the determination of the PCA eigenbasis. The successive rows give the first 4 orders of the PCA Stokes eigenvectors. Here we point out the most relevant features of these plots, which can give us a deeper insight in the formation mechanism of the two He I chromospheric lines. The 1st-order, Q and U eigenvectors show that, to lowest order, the modifications of the scattering linear polarization in the model (due to variations in the radiation anisotropy, and to the magnetic Hanle effect) are positively correlated between the two lines (i.e., both polarization increase or decrease under the same physical mechanism). This fundamental trend is only modified at higher order, as demonstrated by the 3rd-order eigenvectors (4th row of plots) showing a negative correlation between the linear-polarization signatures of the

²One of the determining characteristics of a basis of eigenprofiles for a given line formation problem is its completeness, that is, the property of representing the entire configuration space spanned by the problem. In this sense, any PCA eigenbasis of Stokes profiles can be considered “universal” for the line formation problem at hand. The conditions for which one can trust the completeness of a PCA eigenbasis are the subject of ongoing research.

two lines. At that same order, the Stokes V eigenprofile shows the unmistakable signature of atomic orientation in He I D_3 (due to the alignment-to-orientation mechanism; Landi Degl’Innocenti 1982; Kemp, Macek, & Nehring 1984). It is interesting to note that almost no signal is present for He I 10830 in such case. In other words, if a physical condition existed in a quiescent prominence, such that the resulting Stokes V of He I D_3 were completely due to atomic orientation, then one should expect to see a negligibly small Stokes V signal for the He I 10830 line formed in the same region of the prominence. Therefore, the simultaneous and co-spatial observation of such a peculiar Stokes V profile in He I D_3 *and* of a sizable (Zeeman) Stokes V profile in He I 10830 would imply that the formation regions for the two lines cannot be the same, a possibility that currently is not contemplated by our inversion model. So the 3rd-order, Stokes- V eigenprofile shown in Fig. 1 provides an interesting proxy of non-standard line formation scenarios for the chromospheric lines of He I. On the other hand, the 1st-order, Stokes- V eigenprofile shows that the dominant contribution to Stokes V for both lines, in our model, is in fact due to the Zeeman effect. This is easily explained by the fact that, in our parameter space, we considered field strengths up to 200 G, which are well beyond the level-crossing regime for He I D_3 (30–40 G), at which the alignment-to-orientation mechanism is most effective in the 3^3D term of He I.

In extending our PCA code (López Ariste & Casini 2002) to multi-line inversion, the database creation was modified so that each line’s database is calculated for exactly the same set of magnetic and plasma models. This decision was made in order to minimize the effects of the discrete nature of the PCA database,³ and also to eliminate inversion artifacts due to the presence of ambiguous magnetic configurations (see, e.g., Landi Degl’Innocenti 1982). We then introduced a generalized PCA distance

$$\bar{d}^2 = \sum_{i=1}^N w_i d_i^2, \quad (1)$$

where N is the total number of spectral lines in the model (for the currently adopted model of He I, $N = 6$; see López Ariste & Casini 2002), d_i is the PCA distance for the i -th line, and w_i is a factor ranging between 0 and 1. This last quantity (which at this time is being fixed before the inversion) allows to switch on and off the inversion of a given line, or to give different weights to the lines that are being inverted. The simultaneous PCA inversion of multiple spectral lines thus requires the minimization of the generalized PCA distance defined by eq. (1).

One could alternatively use the eigenprofiles of Fig. 1 for the inversion of simultaneous spectro-polarimetric data in the two chromospheric lines of He I, with the advantage of dealing with only one database of PCA coefficients and one PCA distance for both lines. Since the quality of the inversion is independent of the choice of the eigenprofile basis, this alternate approach is totally legitimate. On the other hand, this would require the preliminary treatment of all spectro-polarimetric data to merge the information from the two lines into fictitious Stokes profiles analogous to those shown in

³In principle, in the case of infinitely dense databases, it would not matter if the databases for two different lines had been calculated on two completely independent set of models.

Fig. 1. An important advantage in keeping separate databases for each line is that it easily allows for the testing of different combinations of lines for magnetic inversion. This is the main argument in favor of our approach to multi-line PCA inversion based on the minimization of a multi-line PCA distance as given by eq. (1).

We preliminarily applied our multi-line PCA inversion code to simultaneous and co-spatial observations of the two chromospheric He I lines in a quiescent prominence, which were acquired in June 2007 at THÉMIS (see Fig. 2). This application to only a few spatial points of the prominence has obviously no relevance for an improved understanding of the magnetic topology of these solar structures. However, the successful fit of these simultaneous, multi-line observations marks an important advance in the spectro-polarimetric diagnostics of scattering polarization, confirming the feasibility of multi-line inversion for magnetic studies of solar prominences. This result strongly advocates for a consistent design of future solar instrumentation that allow multi-line observations of chromospheric lines at the solar limb.

3. Test results

We considered the case of quiescent prominence observations occurring between heights of 0.01 and 0.06 R_{\odot} above the solar limb. The inclination of the line of sight with respect to the radial direction through the prominence was restricted between 85° and 95° in order to avoid the appearance of mixed prominence/filament cases in the synthetic database. The magnetic field strength was limited to $B < 200$ G, without any restriction on the field direction. Finally we assumed a plasma temperature (including micro-turbulence) ranging between 10000 and 15000 K, and an optical depth at line center for the prominence slab ranging between 0.5 and 1.5 for He I 10830. With these parameter intervals, we computed a PCA database of 250 000 models. For the parameter space described above, such a large size of the database is needed in order to mitigate the contribution to the inversion errors coming from the discrete nature of the database. So we can anticipate that the inversion errors in our tests are dominated by the intrinsic uncertainties (ambiguities) in the polarized line formation of the He I lines in prominences.

Next we created three different datasets of synthetic observations, each with 5000 models, to be inverted against the PCA database. One of the datasets spans the same parameter ranges given above. The two other datasets cover a subset of magnetic field strengths, sampling respectively weak fields ($B < 10$ G) and medium fields ($100 \text{ G} < B < 110 \text{ G}$).

Figure 3 shows the scatter plots and histograms of the errors on the inferred magnetic field vector, expressed in the reference system of the observer, for the first dataset. The top set of graphs shows the inversion results using only He I 10830, the second set using only He I D₃, and the bottom set using both lines equally weighted ($w_i = 1$). It is evident that, on average, He I D₃ performs significantly better than He I 10830 in inferring the vector magnetic field information over the entire parameter space. However, He I 10830 helps in reducing the inversion errors, particularly

on the field direction. For the histogram, we report the widths of the error distribution containing 50% and 90% of the inverted models, respectively.

Figures 4 and 5 show similar results for the inversion of the two observation databases created on a restricted range (10 G wide) of magnetic field strengths. We see that He I 10830 provides most of the information that is needed for the inference of weak fields (Fig. 4). Instead, He I D₃ carries more information for larger field strength, as indicated by the results of Fig. 5. This is in general agreement with the fact that the critical field strength for the Hanle effect increases by nearly an order of magnitude going from He I 10830 to He I D₃, where He I 10830 is sensitive to fields between approximately 0.1 and 10 G. It is important to notice that, for all three cases depicted in Figures 3–5, the simultaneous inversions of the two lines give consistently the smallest errors at both the 50% and 90% confidence levels. All the errors shown in the histograms of Figures 3–5 are summarized in Table 1.

In all the inversions, the 90% error on the position angle of the magnetic field projection on the plane of the sky, $\Delta\Phi_B$, is always dominated by errors close to 180°, because of the well-known 180° ambiguity of polarization measurements. We can very clearly distinguish the peaks at 90° in the top set of panels of Figs. 3 and 5. These are determined by the behavior of resonance scattering polarization in the asymptotic regime of the Hanle effect for He I 10830 (Casini, Bevilacqua, & López Ariste 2005). He I D₃ is much less affected by such 90° ambiguity, for this specific range of field strengths. However, it is interesting to note how the simultaneous inversion of He I 10830 and D₃ further reduces the probability of inversion errors associated with the 90° ambiguity.

4. Conclusions

The complexity of magnetic diagnostics in solar prominences, where the observed polarization is dominated by scattering processes, poses particularly strong demands on the robustness of the inversion strategy. One would greatly profit from using multi-line diagnostics, but the feasibility and reliability of such an approach in the case of scattering-dominated, non-LTE, radiative transfer had yet to be demonstrated. In this paper, we took on this task, and considered in particular the simultaneous inversion of the chromospheric He I lines at 587.6 nm and 1083.0 nm.

We performed a statistical study of magnetic-field inference in solar prominences through PCA-based, multi-line inversion, as applied to simultaneous observations of the He I D₃ and 10830. The statistical analysis of the inversion errors on the inferred vector magnetic field was conducted on a database of simulated observations of the two lines. Our analysis confirmed that He I D₃ carries the greatest diagnostic content for typical average fields of quiescent prominences ($B \sim 10$ G and higher), but also demonstrated that the added information carried by the polarization signatures of He I 10830 significantly improves the determination of the magnetic field geometry. On the other hand, He I 10830 is fundamental for the vector measurement of weak magnetic field ($B < 10$ G), although the use of both lines is even more important for the overall reduction of the inversion

errors on both field strength and geometry in this case.

We also demonstrated the applicability of such diagnostics to real data, by inverting some recent simultaneous and co-spatial observations of a quiescent prominence, which were taken with THÉMIS in the two He I chromospheric lines and in $H\alpha$. Although we did not put any emphasis on the interpretation of those observations, the fact that real data are indeed amenable to such multi-line diagnostics allows us to extend the results of our error analysis of multi-line PCA inversion to future observations of quiescent prominences.

We wish to thank A. Asensio Ramos (IAC) for insightful discussions on various statistical aspects of line inversion. B. Lites (HAO) is acknowledged for carefully reading the manuscript and for helpful comments that have improved the presentation of this work. THÉMIS is operated by CNRS-CNR at the Observatorio del Teide of the Instituto de Astrofísica de Canarias (Tenerife, Spain).

REFERENCES

- Berger, T. E., Shine, R. A., Slater, G. L., et al. 2008, *ApJ*, 676, L89
- Casini, R., Bevilacqua, R., & López Ariste, A. 2005, *ApJ*, 622, 1265
- Casini, R., López Ariste, A., Tomczyk, S., & Lites, B. W. 2003, *ApJ*, 598, 67L
- de Toma, G., Casini, R., Burkepile, J. T., & Low, B. C. 2008, *ApJ*, 687, L123
- Elmore, D. F., Casini, R., Card, G. L., et al. 2008, *SPIE*, 7014, 39
- Kemp, J. C., Macek, J. H., & Nehring, F. W. 1984, *ApJ*, 278, 863
- Kuckein, C., Centeno Elliott, R., Martínez Pillet, V., et al. 2009, *A&A*, in press
- Landi Degl’Innocenti, E. 1982, *Sol. Phys.*, 79, 291
- Leroy, J. L. 1977, *A&A*, 60, 79
- López Ariste, A., & Casini, R. 2002, *ApJ*, 575, 529
- Merenda, L., Trujillo Bueno, J., Landi Degl’Innocenti, E., & Collados, M. 2006, *ApJ*, 642, 554
- Paletou, F., & Molodij, G. 2001, in *ASP Conf. Ser. 236, Advanced Solar Polarimetry – Theory, Observation, and Instrumentation*, ed. M. Sigwarth (San Francisco: Astronomical Society of the Pacific), 9
- Paletou, F., López Ariste, A., Bommier, V., & Semel, M. 2001, *A&A*, 375, L39

Querfeld, C. W., Smartt, R. N., Bommier, V., Landi Degl’Innocenti, E., & House, L. L. 1985, Sol. Phys., 96, 277

Semel, M. 1980, A&A, 91, 359

Skumanich, A., & López Ariste, A. 2002, ApJ, 570, 379

Trujillo Bueno, J., Landi Degl’Innocenti, E., Collados, M., Merenda, L., & Manso Sainz, R. 2002, Nature, 415, 403

inverted line(s):			10830		D ₃		10830 + D ₃	
B_{\min}	B_{\max}	ΔX	50%	90%	50%	90%	50%	90%
		B (G)	22.5	97.3	12.3	71.1	10.3	57.0
0 G	200 G	Θ_B (°)	6.1	25.2	4.4	18.1	3.2	12.7
		Φ_B (°)	5.6	179.0	6.0	178.7	3.3	179.1
		B (G)	4.0	99.8	5.6	38.2	2.3	32.5
0 G	10 G	Θ_B (°)	9.1	32.4	10.0	33.9	6.1	23.4
		Φ_B (°)	15.7	177.8	32.4	174.6	8.6	177.8
		B (G)	32.1	83.3	23.9	70.9	18.8	68.2
100 G	110 G	Θ_B (°)	5.7	25.2	4.1	16.9	3.2	11.2
		Φ_B (°)	5.4	179.0	3.7	178.9	2.6	179.0

Table 1: Comparison of the errors at the 50% and 90% confidence level on the inferred values of B , Θ_B , and Φ_B , for single-line and multi-line inversions.

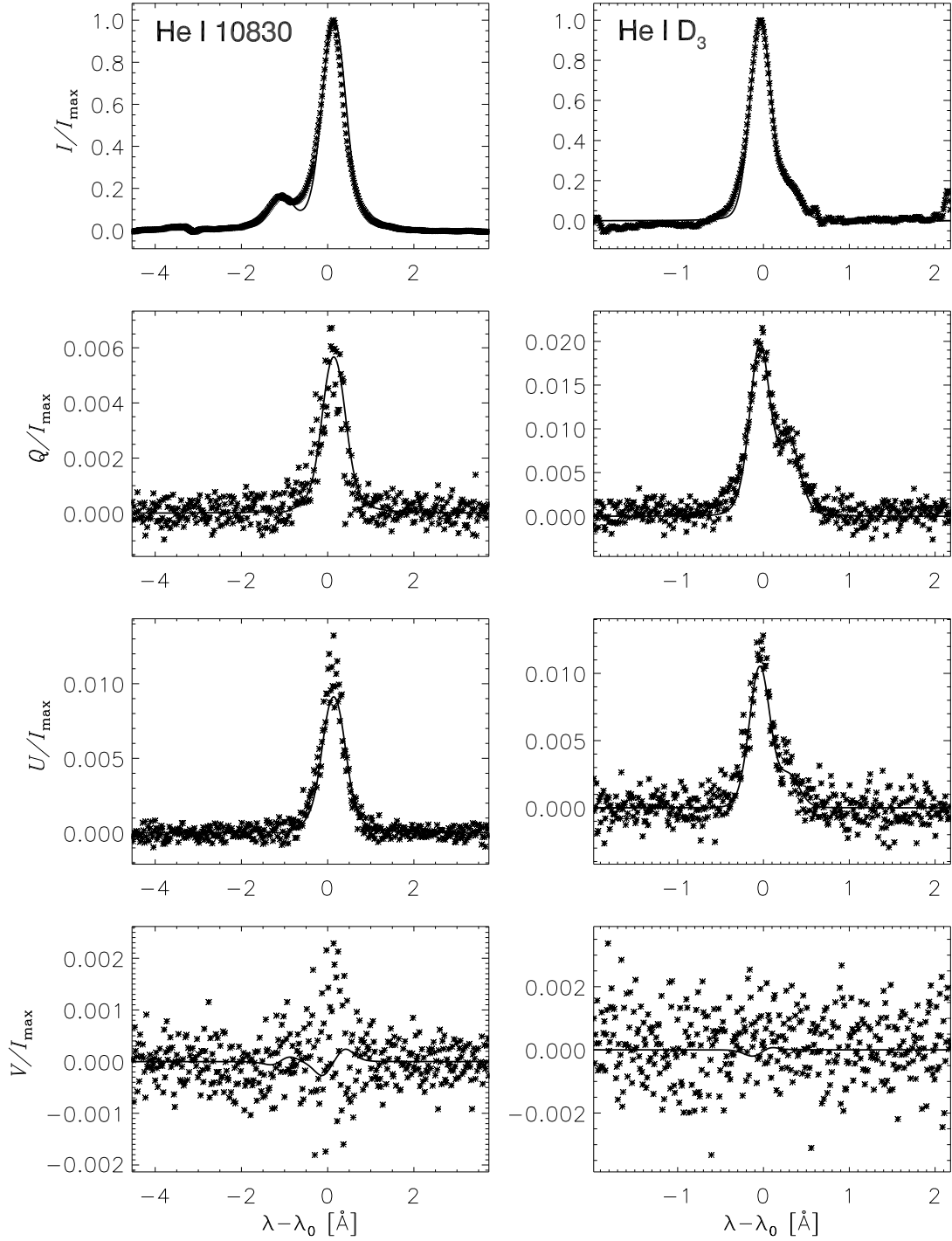


Fig. 2.— Multi-line inversion of simultaneous and co-spatial spectro-polarimetric observations of He I 10830 (left) and D₃ (right) in a quiescent prominence, taken with THÉMIS on June 29, 2007. The inverted vector magnetic field for this example is $B = 3.0$ G, $\vartheta_B = 57.8^\circ$, $\varphi_B = 42.7^\circ$.

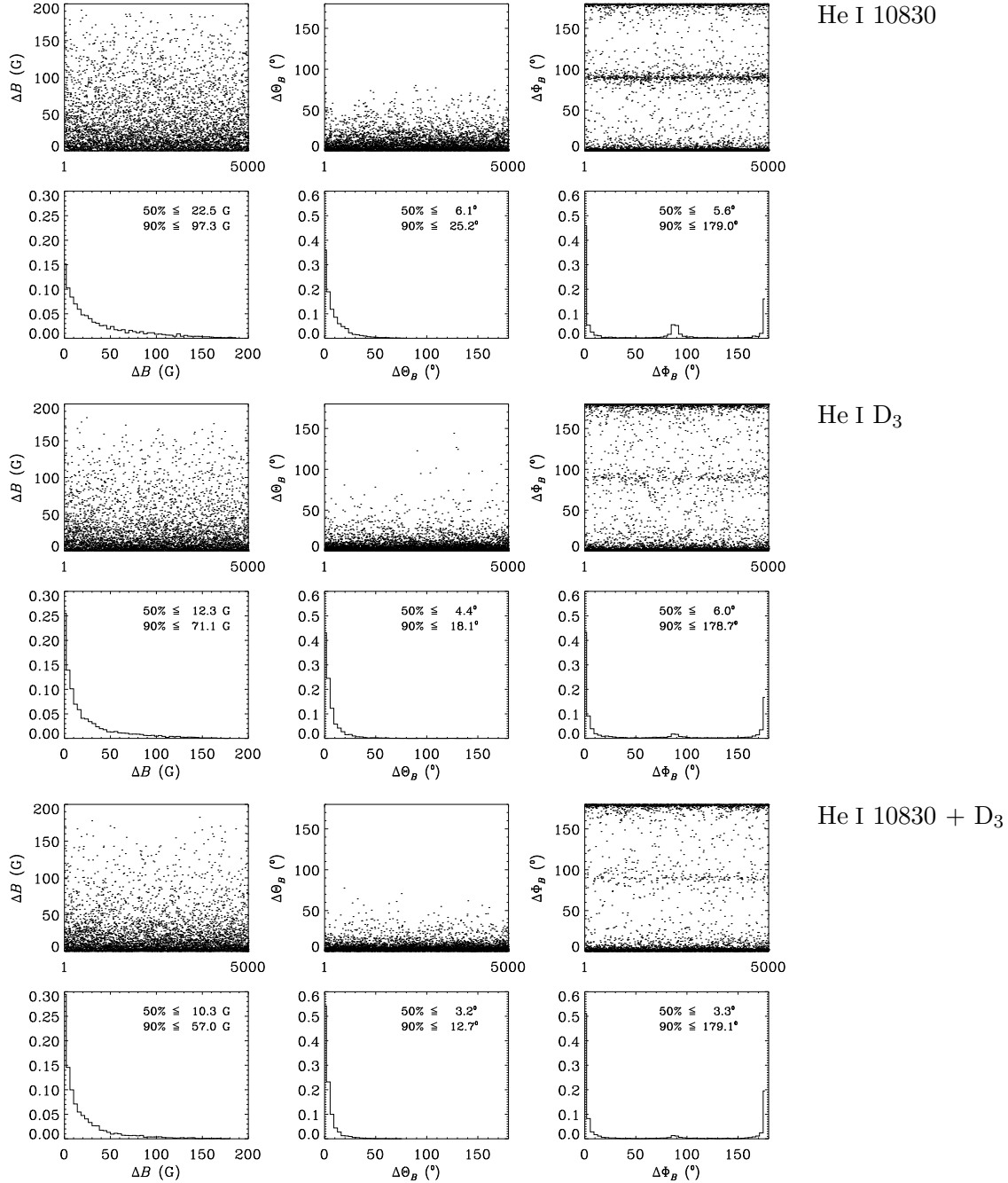


Fig. 3.— Scatter-plot and histogram distributions of the inversion errors on magnetic field strength, B , inclination of the magnetic field along the LOS, Θ_B , and position angle of the magnetic field projection on the POS, Φ_B . The database of 5000 synthetic observations spans the entire range of magnetic strength used in the construction of the inversion database with 150000 models. *Top two rows*: inversion of He I 10830; *middle two rows*: inversion of He I D₃; *bottom two rows*: simultaneous inversion of both lines.

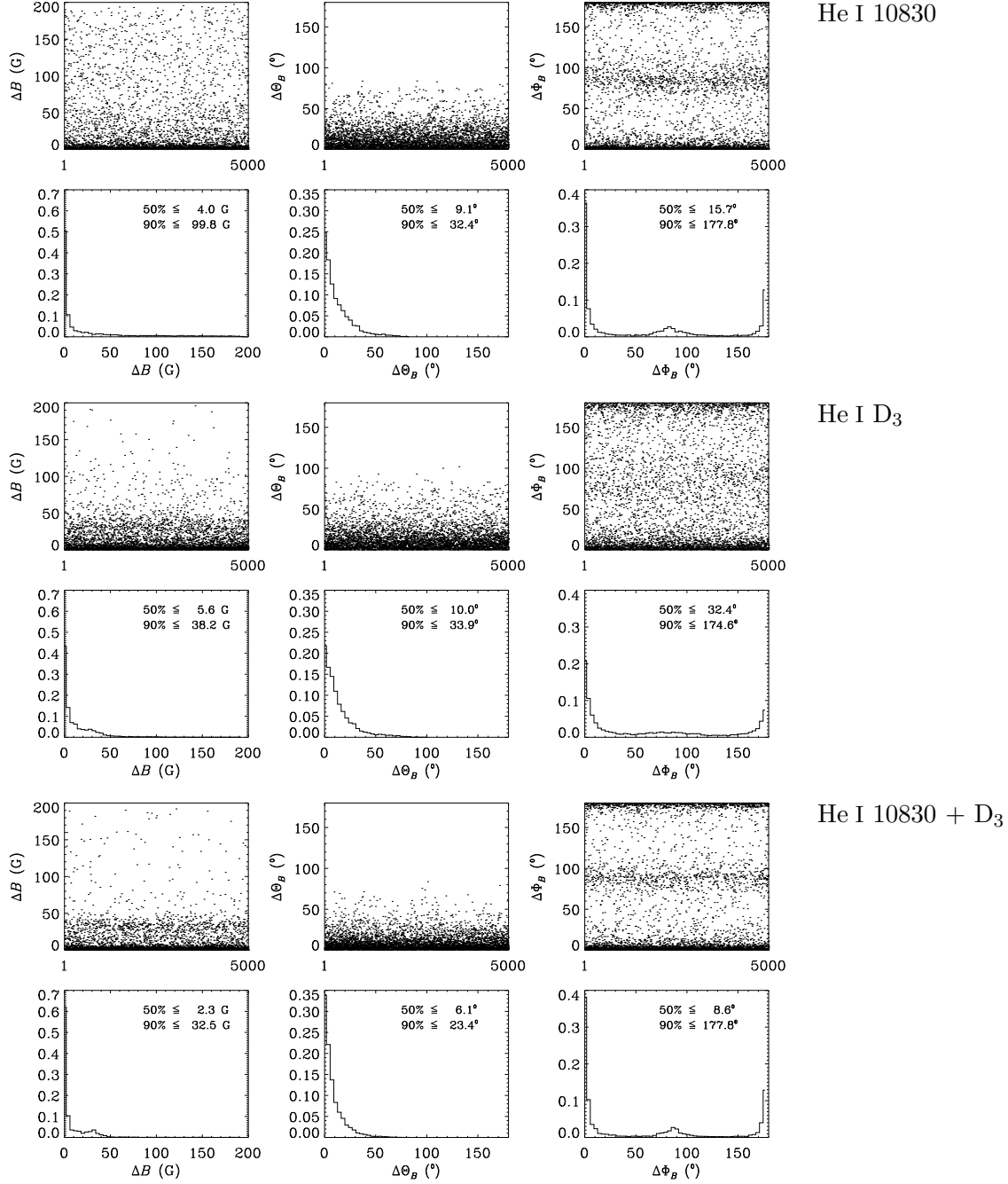


Fig. 4.— Same as Fig. 3, but for a database of simulated observations spanning weak field strengths between 0 and 10 G.

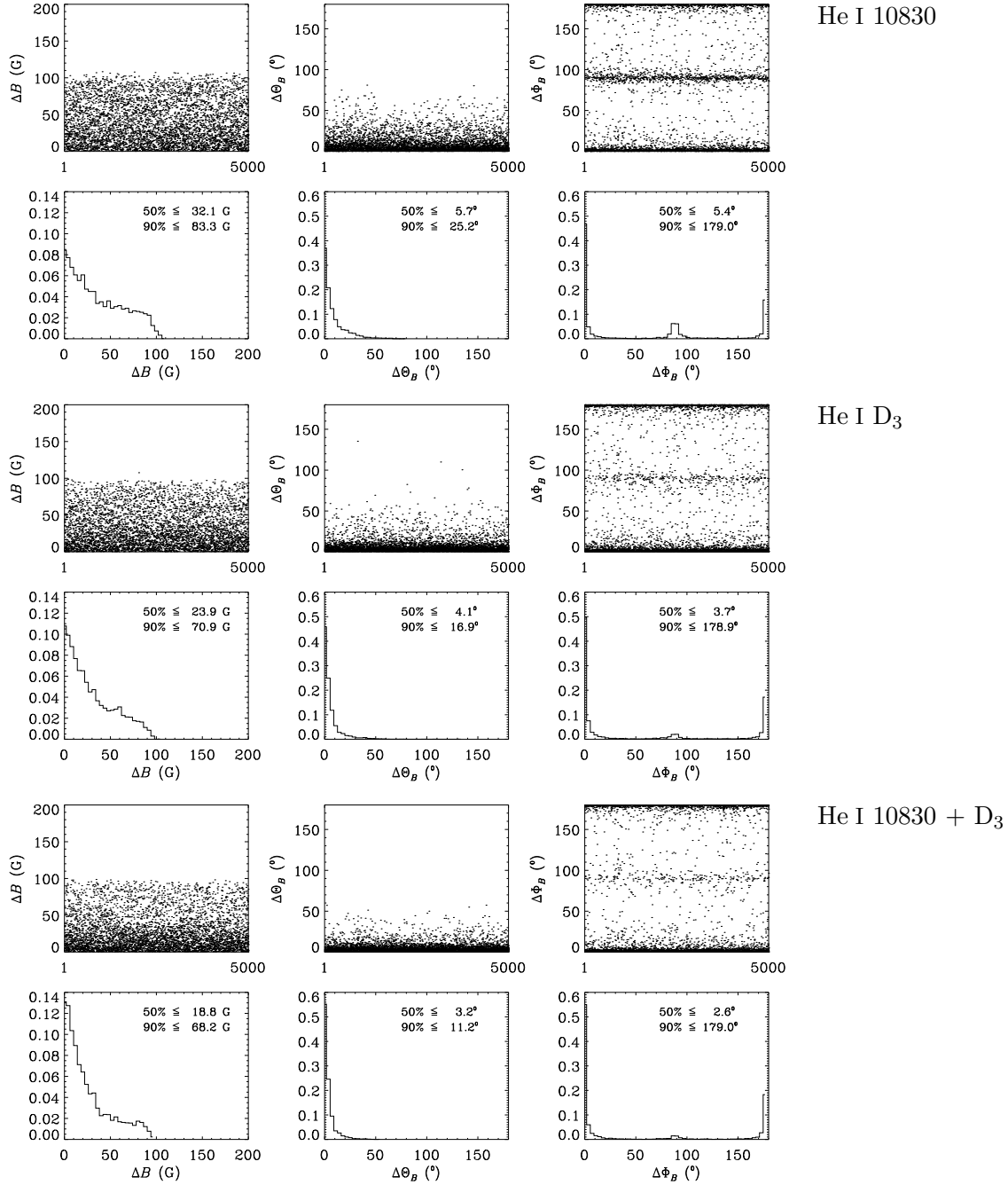


Fig. 5.— Same as Fig. 3, but for a database of simulated observations spanning medium field strengths between 100 and 110 G.